Fault Tolerant Control in a Semi-active Suspension

Juan C. Tudon-Martinez, Rubén Morales-Menéndez, Ricardo A. Ramirez-Mendoza, Olivier Sename, Luc Dugard

HAL Id: hal-00939970
https://hal.science/hal-00939970

Submitted on 31 Jan 2014

Fault Tolerant Control in a Semi-active Suspension [*]

Juan C. Tudón-Martínez [*] Ruben Morales-Menendez [*]
Ricardo Ramírez-Mendoza [*] Olivier Sename [**] Luc Dugard [**]

[*] *Tecnológico de Monterrey, Av. E. Garza Sada 2501, 64849,
Monterrey N.L., México (e-mail: {jc.tudon.phd.mty, rmm,
ricardo.ramirez}@itesm.mx)*
[**] *GIPSA-lab, Control Systems Dept. CNRS-Grenoble INP, ENSE3,
BP 46, F-38402 St Martin d'Hres cedex, France (e-mail:
{olivier.sename, luc.dugard } @gipsa-lab.grenoble-inp.fr)*

Abstract: A Fault Tolerant Control System ($FTCS$) in a Quarter of Vehicle (QoV) model is proposed. The control law is time-varying using a Linear Parameter-Varying (LPV) based controller, which includes two scheduling parameters. One parameter for monitoring the nonlinear behavior of the damper, and another for fault accommodation using a reference model obtained by a state observer of the normal operating regime. The QoV model represents a semi-active suspension, including an experimental magneto-rheological damper model. The $FTCS$ is analyzed when the velocity sensor fails abruptly and the QoV model is susceptible to disturbances in the road profile. Simulation results show the effectiveness of the $FTCS$ in terms of vehicle comfort, suspension deflection and road holding in comparison with a conventional LPV based control system. In the $FTCS$, the comfort index based on the power spectral density is within the desirable bound (1.8) in all range of frequencies, once the sensor fault has occurred; while, the conventional control system deteriorates the comfort 54 %, specially at low frequencies (0-4 Hz). Additionally, the $FTCS$ improves the road holding and suspension deflection indexes, 33% and 39% respectively, when the fault accommodation is considered.

Keywords: Fault-tolerant control, Fault diagnosis, Sensor faults, Semi-active suspension, Automotive control.

1. INTRODUCTION

In modern and advanced technological systems, such as automotive industry, it is necessary to design control systems that consider features of safety and fault tolerance in order to improve the process reliability, Patton (1997). The main objective of a Fault Tolerant Control System ($FTCS$) is to maintain the process performance close to its nominal value and to ensure global stability in the presence of process/instrument failures. A generalized structure of an $FTCS$ can be reviewed in Blanke et al. (2006). Reviews on $FTCS$ (Patton (1997), Jiang (2005), Zhang and Jiang (2008)) present a global classification based on two major groups: those approaches that are designed off-line in robust form, named passive $FTCS$, and those that are based on an automatic control reconfiguration mechanism, named active $FTCS$.

When the number of fault scenarios increases, the passive $FTCS$ can result very conservative and the overall controller performance becomes less and less effective for each fault; whereas, the active $FTCS$ does not have this drawback, Jiang (2005). The control law in the active $FTCS$ demands a reliable Fault Detection and Isolation (FDI) system and an effective reconfigurable control scheme.

The reconfiguration mechanism of switching is used in the Linear Parameter-Varying (LPV) controller, while Model Reference Adaptive Control ($MRAC$) is classified as a tracking mechanism, according to Zhang and Jiang (2008). The control theory based on reference models and LPV systems is gaining importance in $FTCS$ since last decade. For instance, the performance of active and pasive fault-tolerant LPV based control have similar performances according to Sloth et al. (2010). An $FTCS$ is proposed for polytopic LPV systems in Rodrigues et al. (2007), the closed-loop stability under multiple failures is established using a Linear Matrix Inequality (LMI). In Abdullah and Zribi (2009), a model reference control for LPV systems is proposed; however, the controller is not designed to accommodate faults. Similarly, Vargas-Martínez et al. (2010) and Miyasato (2006) proposed an $MRAC$ for an LPV system using a robust H_∞ controller.

In semi-active suspension control systems for vehicles, many researches are focused to improve the vehicle comfort, ensuring its safety and stability. A comparative research in semi-active control strategies for a Magneto-Rheological (MR) suspension is presented in Dong et al. (2010), the sliding mode controller shows the best performance under different road profiles; however, a fuzzy controller has a best road holding. In Savaresi and Spelta (2007), a mixed control based on Sky-Hook (SH) and Acceleration Driven Damping (ADD) framework is proposed

for semi-active dampers, the *SH-ADD* has good comfort performance; however, an innovative controller based on a single-sensor layout, proposed in Spelta et al. (2010), is better in comfort than *SH*, and similar to *SH-ADD*. Based on robust control theory, an *LPV* controller is synthesized to improve the passenger comfort while keeping the road holding index by using an *MR* suspension, Do et al. (2010).

The aforementioned approaches have better performance in comfort than a passive suspension; however, none of them consider the inherent faults in process instrumentation. Otherwise, in a full-vehicle active suspension system, an *FTCS* based on sliding mode theory is proposed by Chamseddine and Noura (2008), good simulation results in an exhaustive analysis are obtained. In Bosche et al. (2009), an *FTCS* for vehicle dynamics is proposed, but the robust controller can not diagnose the faulty component. An *FTCS* on an active suspension system is presented in Yetendje et al. (2007), a set of unknown input observers is proposed to diagnose faults and a linear quadratic regulator is synthesized for each faulty condition. A methodology for controlling the damping ratio of dampers based on estimation of parameters is proposed in Fischer and Isermann (2004), the estimated damper model is used to create a fault signature using parity equations; however, the detected fault is not compensated. In Gáspár et al. (2010), an *FTCS* based on *LPV* control is proposed to guarantee road holding and roll stability in a vehicle model when sensor and actuator faults appear.

This paper proposes an active *FTCS* for a semi-active suspension of a Quarter of Vehicle (*QoV*) which includes an experimental *MR* damper model. The proposed *FTCS* is based on the *LPV* control theory oriented to comfort, by using 2 varying parameters. One for indicating the nonlinearities of the damper, and another one for the fault accommodation using a reference model. The *FDI* module, based on residual generation, provides a scheduling parameter to the *LPV* controller in order to accommodate the fault. The performance of the *FTCS* is compared with a conventional *LPV* controller when sensors of the process fail abruptly.

The outline of this paper is as follows: in the next section, the *QoV* model with an *MR* damper is described. Section 3 presents the proposed *FTCS*. Section 4 shows the simulation tests. A discussion of results is shown in section 5. Finally, conclusions are presented in section 6.

2. Q$_O$V MODEL USING AN MR DAMPER

An experimental *MR* damper model represents the suspension between both masses, Fig. 1. It is assumed that the wheel-road contact is ensured. All variables are described in Table 1.
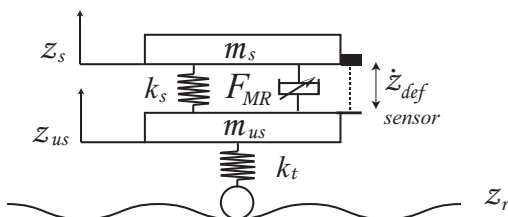

Fig. 1. Model for a *QoV* with a semi-active damper.

Table 1. Definition of Variables.

Variable	Description
c_f	Friction coefficient of the *MR* fluid
$c_{control}$	Maximum value in the controller output
c_{MR}	*MR* damping coefficient
c_p	Passive damping coefficient
c_v	Viscosity coefficient of the *MR* fluid
c_y	Elasticity coefficient of the *MR* fluid
F_{MR}	*MR* damping force
I	Electric current
I_{max}	Maximum electric current allowed
K_o	Observer feedback gain
k_s	Spring stiffness coefficient
k_t	Stiffness coefficient of the wheel tire
m_s	Sprung mass in the *QoV*
m_{us}	Unsprung mass in the *QoV*
u_{sat}	Filtered and bounded controller output
$\dot{z}_\infty$	Absolute of maximum $\dot{z}_{def}$ in the last k samples
$\dot{z}, \dot{z}_{def}$	Damper piston velocity (deflection velocity)
$\dot{z}_{defr}$	Deflection velocity of the reference model
z_r	Road profile (input disturbance)
z_s	Vertical position of the mass m_s
$\dot{z}_s$	Vertical velocity of the mass m_s
$\ddot{z}_s$	Vertical acceleration of the mass m_s
z_{us}	Vertical position of the mass m_{us}
$\dot{z}_{us}$	Vertical velocity of the mass m_{us}
$\ddot{z}_{us}$	Vertical acceleration of the mass m_{us}
ρ	Varying parameter for the *MR* damper hysteresis
ρ_f	Scheduling parameter for the fault accomodation
ρ_{sa}	Scheduling parameter for the current saturation
ρ_{sat}	Scheduling parameter for representing the hysteresis and saturation of the *MR* damper

The system dynamics is given by:

$$m_s\ddot{z}_s = -k_s(z_s - z_{us}) - F_{MR}$$
$$m_{us}\ddot{z}_{us} = k_s(z_s - z_{us}) - k_t(z_{us} - z_r) + F_{MR} \quad (1)$$

The *MR* damper model embedded in the *QoV* is based on Do et al. (2010). The saturation and hysteresis of the *MR* damper is included into the parameter ρ_{sat} (3); where, ρ describes the *MR* phenomenon by a viscous, elasto-plastic, and friction coefficient and ρ_{sa} is the saturated controller output. Thus, the semi-active *MR* damping force is:

$$F_{MR} = c_{MR} \cdot I_{max} \cdot \rho_{sat} + c_p \cdot \dot{z} \quad (2)$$

$$\rho_{sat} = \rho \cdot \rho_{sa} \quad (3)$$

$$\rho_{sa} = tanh(I/c_{control}) \quad (4)$$

$$\rho = c_v\dot{z} + c_y\frac{\dot{z}}{\dot{z}_\infty} + c_f sign(\dot{z})tanh\left(\frac{100}{|(|\dot{z}| - 100)|}\right) \quad (5)$$

$$\dot{z}_\infty = ||(|\dot{z}|)||_{\infty i-k}^{i} = sup\{\dot{z}_{i-k} \ldots \dot{z}_i\} \quad (6)$$

Since I is always positive, the model includes the *sign* function of $\dot{z} = \dot{z}_{def} = (\dot{z}_s - \dot{z}_{us})$ into the parameter ρ for representing the jounce/rebound effects of the damper. A general state-space representation of the *QoV* model can be obtained, rewriting (1) and (2) as:

$$\dot{x}_s = A_s \cdot x_s + B_s \cdot u + B_{s1} \cdot z_r$$
$$y = C_s \cdot x_s + D_s \begin{bmatrix} u \\ z_r \end{bmatrix} + \eta(t) \quad (7)$$

where η is an abrupt sensor fault (gain, bias, breakdown, offset or freeze), u is the saturated controller output and,

$$y = \dot{z}_{def}, \ C_s = [\, 0 \ 1 \ 0 \ -1\,], \ D_s = [\, 0 \ 0\,]$$

$$B_s = \begin{bmatrix} 0 \\ \dfrac{-c_{MR} \cdot \rho}{m_s} \\ 0 \\ \dfrac{c_{MR} \cdot \rho}{m_{us}} \end{bmatrix}, \ B_{s1} = \begin{bmatrix} 0 \\ 0 \\ 0 \\ \dfrac{k_t}{m_{us}} \end{bmatrix}, \ x_s = \begin{bmatrix} z_s \\ \dot{z}_s \\ z_{us} \\ \dot{z}_{us} \end{bmatrix}$$

$$A_s = \begin{bmatrix} 0 & 1 & 0 & 0 \\ \dfrac{-k_s}{m_s} & \dfrac{-c_p}{m_s} & \dfrac{k_s}{m_s} & \dfrac{c_p}{m_s} \\ 0 & 0 & 0 & 1 \\ \dfrac{k_s}{m_{us}} & \dfrac{c_p}{m_{us}} & \dfrac{-k_s - k_t}{m_{us}} & \dfrac{-c_p}{m_{us}} \end{bmatrix}, \ u = I_{max}\rho_{sa}$$

3. FAULT-TOLERANT CONTROL DESIGN

In the QoV system defined by (7), it is assumed that $\dot{z}_{def}$ is measured by a linear velocity sensor, Fig. 1. Figure 2 shows a block diagram of the $FTCS$ approach; the controller inputs are $\dot{z}_{def}$ and 2 varying parameters: ρ_{sat}^* includes the nonlinearities of the damper and ρ_f quantifies the fault by using a reference model of the QoV. The fault is implemented in additive form, called *soft* fault.
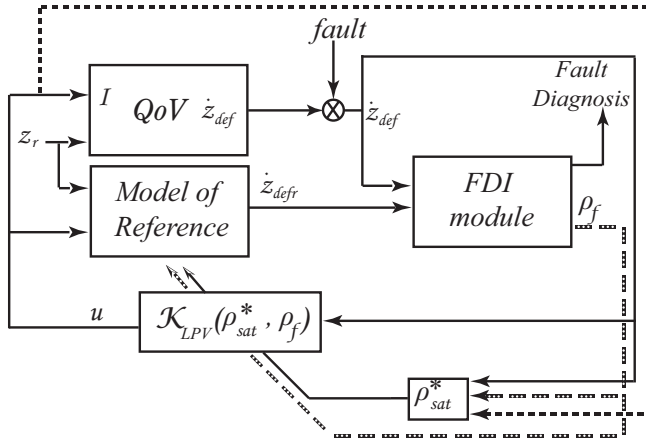

Fig. 2. Proposed *FTCS* structure applied on a *QoV*.

3.1 FDI using a reference model

The *FDI* module is based on a residual generation. The reference model (baseline process) was obtained by a state observer in the overall operating regime of the process, by including the nonlinearities of the *MR* damper:

$$\dot{\tilde{x}}_s = A_s \cdot \tilde{x}_s + B_s \cdot u + B_{s1} \cdot z_r + K_o(y - \hat{y})$$
$$\hat{y} = C_s \cdot \tilde{x}_s = \dot{z}_{defr} \tag{8}$$

where, K_o is the observer feedback matrix used to reduce the differences between the reference model and the process. The pole placement method is used to find K_o which guarantees the convergence speed and observer stability.

The residual r is computed as: $r = \dot{z}_{defr} - \dot{z}_{def}$. When the residual is close to zero, the process is free of faults, while any change in r represents a faulty scheme. In the *FDI* module, ρ_f, which is bounded and available online, is generated to achieve the fault accommodation by including any faulty scheme in the control system. In (9), ϵ is a constant different to zero used to avoid ambiguities, by assuming a resolution in $\dot{z}_{def}$ of 1 mm/s, $\epsilon = 1 \times 10^{-4}$.

$$\rho_f = \frac{\dot{z}_{defr} + \epsilon}{\dot{z}_{def} + \epsilon} \in [-4, 4] \tag{9}$$

ρ_f expresses the ratio between the desired deflection velocity and the *measured* signal; its range (peak to peak) is defined by simulation with different faults. If $\dot{z}_{defr}$ is higher than the measurement, ρ_f will be the factor that must multiply the failed signal $\dot{z}_{def}$ in (17) for accommodating the fault. If the velocity sensor is free of faults, $\rho_f = 1$, the *MR* force is obtained in normal form. False positives and negatives strongly depend on the accuracy of the reference model; thus, it is necessary to use a reliable model in order to have a low false alarm rate. Using ρ_f defined in (9), A_s and ρ are rewritten as:

$$A_s(\rho_f) = \begin{bmatrix} 0 & 1 & 0 & 0 \\ \dfrac{-k_s}{m_s} & \dfrac{-c_p \cdot \rho_f}{m_s} & \dfrac{k_s}{m_s} & \dfrac{c_p \cdot \rho_f}{m_s} \\ 0 & 0 & 0 & 1 \\ \dfrac{k_s}{m_{us}} & \dfrac{c_p \cdot \rho_f}{m_{us}} & \dfrac{-k_s - k_t}{m_{us}} & \dfrac{-c_p \cdot \rho_f}{m_{us}} \end{bmatrix} \tag{10}$$

$$\rho(\rho_f) = c_v \dot{z}\rho_f + c_y \frac{\dot{z}\rho_f}{\dot{z}\rho_{f\infty}} + c_f sign(\dot{z})tanh\left(\frac{100}{|(|\dot{z}\rho_f| - 100)|}\right) \tag{11}$$

In presence of a fault, $\rho(\rho_f)$ will be blind to the failure because ρ_f will accommodate the value of $\dot{z}$. Thus, ρ_{sat} (3) is redefined to include the fault as:

$$\rho_{sat}^* = \rho(\rho_f) \cdot \rho_{sa} \tag{12}$$

3.2 Synthesis of the LPV controller

LPV Modelling. The *LPV* structure of the QoV model can be obtained as follows. First, a low pass filter must be added to the QoV model for matching the controller actuation with the damper time response; this filter allows to build a proper model structure for the *LPV* based controller synthesis, Poussot-Vassal et al. (2008). A filter with bandwidth of 25 Hz was used for ensuring the time response of the *MR* damping force (~ 40 ms):

$$\mathcal{F}: \begin{bmatrix} \dot{x}_f \\ u_f \end{bmatrix} \begin{bmatrix} A_f & B_f \\ C_f \rho_{sat}^* & 0 \end{bmatrix} \begin{bmatrix} x_f \\ u \end{bmatrix} \tag{13}$$

Second, a saturation function must be designed as:

$$u_{sat} = \begin{cases} I_{max} & if \quad u_f >> I_{max} \\ u_f & if \quad 0 \le u_f \le I_{max} \\ 0 & if \quad u_f << 0 \end{cases} \tag{14}$$

The filtered-saturated manipulation is approximated as,

$$u_{MR} \cong C_f x_f \cdot \rho_{sat}^* \in [0 - 2.5]A \tag{15}$$

The new structure (16) takes into account the saturation and semi-activity of the damper in the controller output; this signal includes the varying parameter instead the matrix B which only contains the filtering property. Figure 3 shows a block diagram of this new structure.

$$\dot{x}_{sf} = A(\rho_{sat}^*, \rho_f) \cdot x_{sf} + B \cdot u_{MR} + \begin{bmatrix} B_{s1} \\ 0 \end{bmatrix} \cdot z_r \tag{16}$$
$$y = [\, C_s \ 0\,] \cdot x_{sf} + \eta(t)$$

$$x_{sf} = \begin{bmatrix} x_s \\ x_f \end{bmatrix}, \ A(\rho_{sat}^*, \rho_f) = \begin{bmatrix} A_s(\rho_f) & \rho_{sat}^* B_s C_f \\ 0_{1\times 4} & A_f \end{bmatrix}, \ B = \begin{bmatrix} 0_{4\times 1} \\ B_f \end{bmatrix}$$
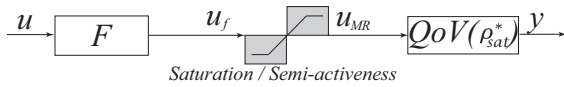
Fig. 3. QoV model with a semi-active saturated input.

Design of a Polytopic LPV Controller. The *MR* damping force described in (2) can be redefined by adding the scheduling parameter ρ_f for the fault accommodation as:

$$F_{MR} = c_{MR} \cdot I_{max} \cdot \rho_{sat}^* + c_p \cdot \dot{z}_{def} \cdot \rho_f$$
$$\rho_{sat}^* \in [0, 500] \tag{17}$$

The span of ρ_{sat}^* is defined experimentally, Fig. 5.

LPV control theory deals with nonlinearities of the process and allows to obtain a varying controller through linear changes of the model parameters. The *LPV* based controller can be obtained through the interpolation of a polytope whose vertices are Linear Time-Invariant (*LTI*) controllers. The controller design is oriented to comfort assuming that the wheel-road contact is ensured.

Since the *LPV* model of the *QoV* depends on 2 varying parameters defined in (9) and (12), a polytope of 4 *LTI* controllers is designed using the H_∞ control framework. This robust control theory is based on the synthesis of a stable controller that minimizes the impact of the disturbance z_r and model uncertainties on the controlled output. The *LPV* controller is defined as an optimization problem solved by an *LMI*, Poussot-Vassal et al. (2008). Figure 4 describes the structure for designing the H_∞ controller. The weighting functions, based on a priori knowledge of the performance objectives, are designed to ensure stability without performance degradation as,

$$W_{\ddot{z}_s} = \frac{K_s \omega_s^2}{s^2 + 2\zeta \omega_s s + \omega_s^2}, \ W_{z_{us}} = \frac{K_{us}\omega_{us}}{s + \omega_{us}}, \ W_{z_r} = 3 \times 10^{-2}$$

where $W_{\ddot{z}_s}$ allows to reduce the amplification of $\ddot{z}_s$ for
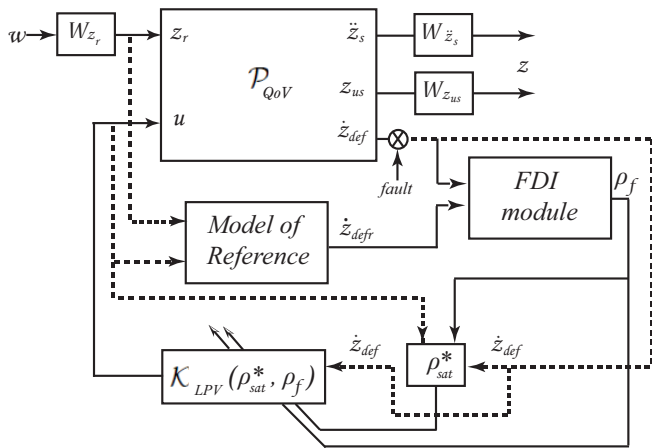

Fig. 4. H_∞ controller for a *LTI* model of a *QoV*.

achieving the desired comfort, $W_{z_{us}}$ is shaped to ensure the road holding and W_{z_r} increases the sensitivity to the road profile. Taking into account the control specifications, the generalized system $\mathcal{P}$ for the *LPV* control synthesis is,

$$\dot{x}_{sf} = A(\rho_{sat}^*, \rho_f) \cdot x_{sf} + B \cdot u_{MR} + \begin{bmatrix} B_{s1} \\ 0 \end{bmatrix} \cdot W_{z_r} \cdot w$$

$$\begin{bmatrix} \ddot{z}_s \\ z_{us} \end{bmatrix} = C_1(\rho_{sat}^*, \rho_f) \cdot x_{sf}$$

$$z = \begin{bmatrix} \ddot{z}_s \ z_{us} \end{bmatrix}^T \cdot \begin{bmatrix} W_{\ddot{z}_s} & 0 \\ 0 & W_{z_{us}} \end{bmatrix} = \begin{bmatrix} \ddot{z}_s \ z_{us} \end{bmatrix}^T \cdot W$$

$$y = C_2 \cdot x_{sf} \tag{18}$$

where $C_1(\rho_{sat}^*, \rho_f) = [\, C_{s1}(\rho_f) \ \rho_{sat}^* D_{s1} C_f \,]$ and,

$$D_{s1} = \begin{bmatrix} \dfrac{-1}{m_s} \\ 0 \end{bmatrix}, \ C_{s1}(\rho_f) = \begin{bmatrix} \dfrac{-k_s}{m_s} & \dfrac{-c_p\rho_f}{m_s} & \dfrac{k_s}{m_s} & \dfrac{c_p\rho_f}{m_s} \\ 0 & 0 & 1 & 0 \end{bmatrix}$$

$$C_2 = [\, C_{s2} \ 0 \,], \ C_{s2} = [\, 0 \ 1 \ 0 \ -1 \,]$$

3.3 Hurwitz stability criterion

For *LPV* control synthesis, the Hurwitz criterion consists in placing poles of the closed-loop system into a region bounded by a polytope. Considering two varying parameters, the *LPV* polytopic controller is given as,

$$\mathcal{K}_{LPV}(\rho) = \Sigma_{i=1}^4 \alpha_i \begin{bmatrix} Ac_i & Bc_i \\ Cc_i & Dc_i \end{bmatrix} \tag{19}$$

where,

$$\alpha_i(\rho) := \frac{\prod_{k=1}^2 |\rho_k - \mathcal{K}(w_i)_k|}{\prod_{k=1}^2 (\bar{\rho}_k - \underline{\rho}_k)}, i = 1, \dots, 4 \tag{20}$$

α_i is the weight of the i *LTI* controller ($\Sigma_{i=1}^4 \alpha_i(\rho) = 1$) and $\mathcal{K}(w_i)$ is the i vertex of the polytopic system. The closed-loop system of a generalized *LTI* system described in (18) with a *LTI* controller defined in (19) is given by,

$$G(\mathcal{P}, \mathcal{K}) : \begin{bmatrix} \dot{\xi} \\ z \end{bmatrix} = \begin{bmatrix} \mathcal{A} & \mathcal{B} \\ \mathcal{C} & \mathcal{D} \end{bmatrix} \begin{bmatrix} \xi \\ w \end{bmatrix} \tag{21}$$

where, $\xi = [x_{sf}^T \ x_c^T]$ (x_c is the controller state), $\mathcal{D} = 0$ and,

$$\mathcal{A} = \begin{bmatrix} A + BD_cC_2 & BC_c \\ B_cC_2 & A_c \end{bmatrix} \ \mathcal{B} = \begin{bmatrix} B_{s1}W_{z_r} \\ 0_{2\times1} \end{bmatrix} \ \mathcal{C} = \begin{bmatrix} C_1 W & 0_{2\times1} \end{bmatrix}$$

The aim is to find a Lyapunov function X that satisfies,

$$V(\xi) = \xi^T X \xi, \tag{22}$$

where, V must be positive defined; and its derivative,

$$\dot{V}(\xi) = \xi^T (\mathcal{A}^T X + X\mathcal{A})\xi, \tag{23}$$

must be negative defined. By solving the *LMIs* in X for each vertex of the polytopic closed-loop system, the asymptotical stability is ensured (making $\mathcal{A}$ Hurwitz).

4. SIMULATION TESTS

Based on the QoV model, *MR* damper model and *LPV* controller, several simulations were implemented. The QoV model parameters described in eqn. (1) have been identified from a commercial vehicle, Table 2.

Table 2. QoV model parameters.

Parameter	Value	Parameter	Value
m_s	387 (Kg)	m_{us}	139.5 (Kg)
k_s	37,300 (N/m)	k_t	295,200 (N/m)

The model coefficients in the jounce and rebound effect of the shock absorber are shown in Table 3; they were identified based on a standard test (*chirp* of 25 mm of amplitude at [0.5-15] Hz). Table 4 shows the parameters of the weighting functions in the controller, the cut frequencies

Table 3. MR damper model coefficients.

Coefficient	$\dot{z}_{def} > 0$	$\dot{z}_{def} < 0$	units
c_v	0.257	0.089	s/mm
c_y	-9.3	5.6	-
c_f	0.9158	0.5461	mm/s
c_{MR}	6.481	3.62	N/A
c_p	0.8	0.8	Ns/mm
$c_{control}$	25	25	-
I_{max}	2.5	2.5	A
k	228	228	-

Table 4. LPV controller parameters.

Parameter	Value	Parameter	Value
K_s	1	ω_{us}	$53.4(rad/s)$
ζ	0.7	K_{us}	1
ω_s	$15.7(rad/s)$		

have been selected according to the resonance frequencies of the sprung (~ 2.5 Hz) and unsprung mass (~ 8.5 Hz).

Figure 5 (top plot) compares the damper model and experimental data generated from an MR damper which has continuous actuation between 0-2.5 A with a range of damping force of $\pm$ 4000 N and stroke of ± 40 mm; while bottom plot shows the ρ^*_{sat} range.
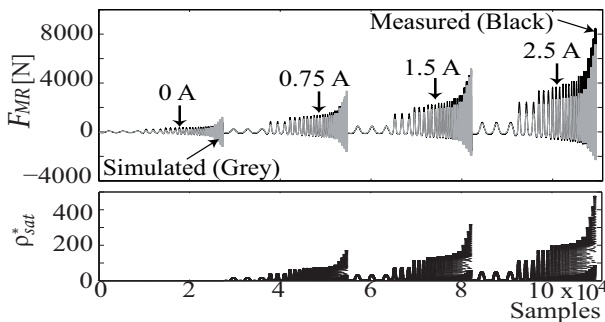

Fig. 5. Comparison of the experimental and modeled MR damping force at different electric currents (top); behavior of ρ^*_{sat} in the identification test (bottom).

The performance specification for comfort at low frequencies, [0-5] Hz, establishes that the maximum gain of the frequency response z_s/z_r must be bounded by 1.8, Poussot-Vassal et al. (2008). A human can feel dizziness and sickness caused by sudden motions. The comfort at high frequencies, [5-20] Hz, is evaluated by $\ddot{z}_s/z_r$; although human is not sensitive at this frequencies, is desirable that the gain be low. A good road holding is considered when the maximum gain of $\frac{z_{us} - z_r}{z_r}$ is limited to 2.5 for low disturbances ($z_r < 3cm$) from 0 to 20 Hz, while the life cycle of the damper is preserved when z_{def} is low.

The $FTCS$ is compared with a conventional LPV based controller in order to analyze its effectiveness when a disturbance on the road is presented and the velocity sensor fails. An abrupt sensor fault such as gain, bias, breakdown, offset or freeze has been implemented; and z_r is a signal *chirp* of 2 cm from 0.5 to 20 Hz. The conventional controller synthesis does not include the fault accommodation property provided by the FDI module.

5. RESULTS AND DISCUSSION

An abrupt fault of magnitude 4σ is implemented in the $\dot{z}_{def}$ sensor at $t = [1.25 - 3.75]$ s. Figure 6 shows that the fault detection and ρ_f computing occur simultaneously.
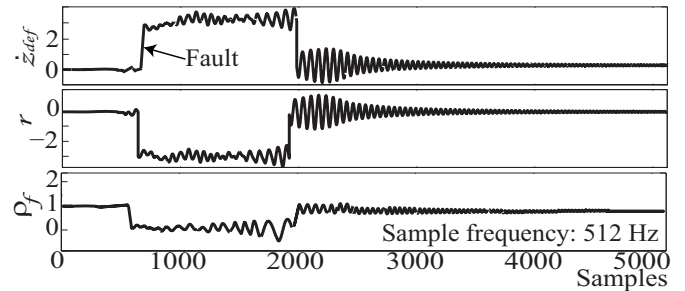

Fig. 6. Detection of a sensor fault in the QoV.

A pseudo-Bode plot tests the frequency response of the control system, Poussot-Vassal et al. (2008); it shows the maximum gain of the system for each excitation frequency. Figure 7 presents the frequency response of z_s/z_r, the conventional LPV based controller shows a gain greater than the acceptable limit (1.8) at frequencies lower than 4 Hz, while the $FTCS$ ensures the comfort in the entire range of frequencies even a fault sensor has occurred.
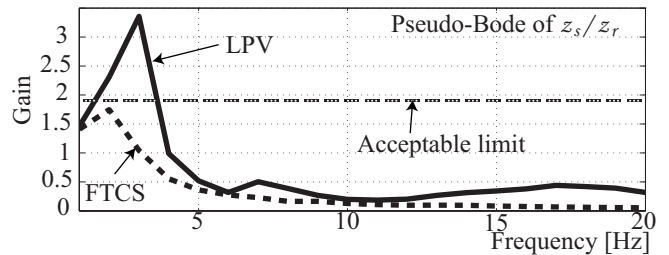

Fig. 7. Comparison of the passenger comfort index between the conventional controller and the proposed $FTCS$.

The acceleration of the sprung mass is also deteriorated from 0 - 12 Hz when the fault is not accommodated, mainly at the resonance frequency of m_s, 2.5 Hz, Fig. 8.
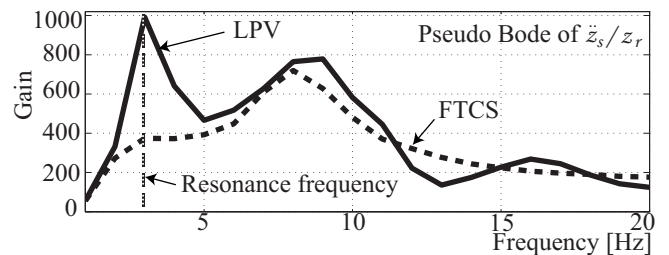

Fig. 8. Comparison of $\ddot{z}_s$ between both control strategies.

The road holding is analyzed in the Fig. 9. Practically, both control systems satisfy the limit (2.5); however, the LPV controller shows greater gain at low frequencies (2-5 Hz), i.e the wheel deflection is increased. Similarly, the suspension deflection (z_{def}) is considerably bigger at low frequencies when the fault can not be accommodated; this reduces the lifetime of the shock absorber.

Table 5 shows the Root Mean Square (RMS) of the variables z_s, $\ddot{z}_s$, $z_{us} - z_r$ and z_{def} for comparing the transient response of both approaches when the sensor fails. All
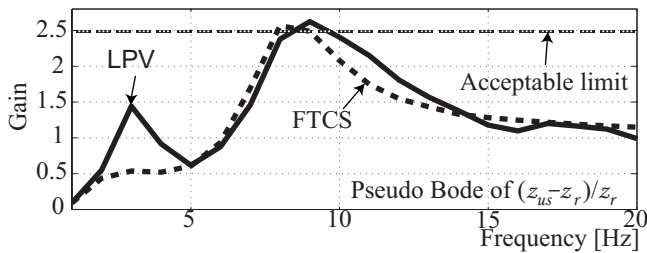
Fig. 9. *PSD* of the road holding index in both controllers.

control objectives are better in the *FTCS*, specially the comfort because the *RMS* of z_s is reduced to 2.6 cm (54%).

Table 5. Comparison of *RMS* index.

Control Approach	z_s (cm)	$\ddot{z}_s$ ($\frac{m}{s^2}$)	$z_{us} - z_r$ (cm)	z_{def} (cm)
FTCS	2.2	8.1	1.8	2.6
LPV conventional	4.8	9.5	2.7	4.3

If the control system presents new/unknown sensor faults, the *FDI* module must be capable to detect this failure since any deviation from the reference model is considered as abnormal condition, moreover if the fault effect is bounded by the span of ρ_f, the fault will be compensated. However, the *LPV* controller must increase its conservatism in order to take into account the uncertainty of the unknown fault, thus the overall controller performance becomes less effective for each fault.

6. CONCLUSIONS

A Fault Tolerant Control System (*FTCS*) of a semi-active suspension in a Quarter of Vehicle (*QoV*) model is proposed. The proposed *FTCS*, considered as an active scheme, is based on a Fault Detection and Isolation (*FDI*) module which accommodates the fault on the controller reconfiguration by using the Linear Parameter-Varying (*LPV*) control theory. Two scheduling parameters are included in the *LPV* control design, one incorporates the nonlinear behavior (saturation and semiactiveness) of a Magneto-Rheological (*MR*) damper and the other is used for the fault accommodation; since both scheduling variables depend on the measured signal ($\dot{z}_{def}$), they can be calculated. The scheduling parameter that accommodates the malfunction is provided by the *FDI* system as a ratio between the output of a reference model and the process. The reference model is the process in normal operating conditions. A comparison between the *FTCS* and a conventional *LPV* controller shows the effectiveness of *FTCS* for accommodating sensor faults.

Simulation results in the frequency response show that the fault deteriorates the comfort (54%) when this is not accommodated, mainly at low frequencies (0-5 Hz); the comfort index of the conventional controller overshoots the recommended limit. Similarly, the *FTCS* shows lower acceleration in the sprung mass in almost all frequency automotive range. On the other hand, the road holding index shows that the *FTCS* can increase the safety (33%) in the vehicle when a *soft* fault in the $\dot{z}_{def}$ sensor occurs, while the suspension deflection index represents a 39% of improvement in the lifetime of the damper, specially at low frequencies.

REFERENCES

Abdullah, A. and Zribi, M. (2009). Model Reference Control of LPV Systems. *J. Franklin I.*, 346, 854–871.

Blanke, M., Kinnaert, M., Lunze, J., and Staroswiecki, M. (2006). *Diagnosis and Fault-Tolerant Control.* Springer, 2nd Ed., Berlin.

Bosche, J., Hajjaji, A., and Rabhi, A. (2009). Actuator Fault-Tolerant Control for Vehicle Dynamics. In 7th *Safeprocess, Spain*, 1103–1108.

Chamseddine, A. and Noura, H. (2008). Control and Sensor Fault Tolerance of Vehicle Active Suspension. *IEEE Trans. on Control Systems Tech.*, 16(3), 416–433.

Do, A., Spelta, C., Savaresi, S., Sename, O., Dugard, L., and Delvecchio, D. (2010). An LPV Control Approach for Comfort and Suspension Travel Improvements of Semi-Active Suspension Systems. In 49th *IEEE Conf. on Decision and Control, USA*, 5560–5565.

Dong, X., Yu, M., Liao, C., and Chen, W. (2010). Comparative Research on Semi-Active Control Strategies for Magneto-rheological Suspension. *Nonlinear Dynamics*, 59, 433–453.

Fischer, D. and Isermann, R. (2004). Mechatronic Semi-active and Active Vehicle Suspensions. *Control Eng. Practice*, 12, 1353–1367.

Gáspár, P., Szabó, Z., and Bokor, J. (2010). LPV Design of Fault-tolerant Control for Road Vehicles. In *Conf. on Control and Fault Tolerant Systems, France*, 807–812.

Jiang, J. (2005). Fault-tolerant Control Systems -An Introductory Overview. *ACTA Automatica*, 31, 161–174.

Miyasato, Y. (2006). Model Reference Adaptive Control of Polytopic LPV Systems - An Alternative Approach to Adaptive Control. In *Int. Symp. on Intelligent Control, Germany*, 2012–2017.

Patton, R. (1997). Fault Tolerant Control: The 1997 Situation. In 3rd *Safeprocess, England*, 1033–1055.

Poussot-Vassal, C., Sename, O., Dugard, L., Gáspár, P., Szabó, Z., and Bokor, J. (2008). A New Semi-active Suspension Control Strategy through LPV Technique. *Control Eng. Practice*, 16, 1519–1534.

Rodrigues, M., Theilliol, D., Aberkane, S., and Sauter, D. (2007). Fault Tolerant Control Design for Polytopic LPV Systems. *Int. J. AMCS*, 17(1), 27–37.

Savaresi, S. and Spelta, C. (2007). Mixed Sky-hook and ADD: Approaching the Filtering Limits of a Semi-active Suspension. *J. of Dynamic Systems, Measurement and Control*, 169, 382–392.

Sloth, C., Esbensen, T., and Stoustrup, J. (2010). Active and Pasive Fault-Tolerant LPV Control of Wind Turbines. In *American Control Conf., USA*, 4640–4646.

Spelta, C., Savaresi, S., and Fabbri, L. (2010). Experimental Analysis of a Motorcycle Semi-active Rear Suspension. *Control Eng. Practice*, 18, 1239–1250.

Vargas-Martínez, A., Puig, V., Garza-Castañón, L., and Morales-Menendez, R. (2010). MRAC + H_∞ Fault Tolerant Control for Linear Parameter Varying Systems. In *SysTol 2010, France*, 94–99.

Yetendje, A., Seron, M., and Dona, J.D. (2007). Diagnosis and Actuator Fault Tolerant Control in Vehicle Active Suspension. In *ICIAFS'07, Melbourne, VIC*, 153–158.

Zhang, Y. and Jiang, J. (2008). Bibliographical Review on Reconfigurable Fault-tolerant Control Systems. *Annual Reviews in Control*, 32, 229–252.